Chemical reaction strengthening of Al/TiC metal matrix composites by isothermal heat treatment at 913 K

R. Mitra, M. E. Fine, and J. R. Weertman
Department of Materials Science and Engineering, Northwestern University, Evanston, Illinois 60208-3108

(Received 9 October 1992; accepted 23 April 1993)

The effect of solid state heat treatment at 913 K on extruded XD Al/TiC metal matrix composite with 0.7 and 4.0 μm particle sizes has been investigated. The interfaces between Al and TiC after extrusion were atomically abrupt, as observed by HRTEM. On holding at 913 K, the composite with submicron particle size showed substantial changes in the phases present due to reaction between Al and TiC at 913 K. The stable reaction products are Al_3Ti and Al_4C_3. A substantial increase in Young's modulus occurs. The room and elevated temperature strength and hardness of the composite with submicron particles also increase significantly with time of heat treatment, but at the expense of ductility. The effect of heat treatment over the time range investigated is limited to the interfaces for the 4.0 μm TiC particle size composite due to longer diffusion paths.

I. INTRODUCTION

Aluminum based metal matrix composites are of increasing interest because of their stiffness to weight ratios and wear resistance.[1] For high temperature applications and because of possible reaction during fabrication, the thermodynamic stability of the reinforcement phase with respect to reaction with the matrix is of great significance. In many cases such as Ti/SiC or Al/SiC composites, formation of reaction products at the interface results in degradation of ductility and fracture toughness.[2,3]

Recently, theoretical[4–8] and experimental[9–11] studies on the Al–Ti–C system have been reported. *In situ* Al/TiC composites have been prepared by several research groups[12–14] and the XD processing technique is of particular interest. The Al and TiC phases have been reported to be thermodynamically stable at the processing temperature which is well above that of molten aluminum.[15] The interfaces in XD Al/TiC composites are atomically abrupt[16]; the atom planes of each phase extend to the interface. However, in a theoretical work, Yokokawa *et al.*[8] predicted that Al and TiC cannot coexist in thermodynamic equilibrium at low temperatures like 973 K. Ternary phase diagrams have been drawn at different temperatures above the melting point of Al,[4,5,17] but only one publication has reported appearance of Al_3Ti and Al_4C_3 in an Al/TiC composite on isothermal solid state heat treatment (873 K). No explanation of the conditions and no thermodynamic data were given.[11] The phases produced and the kinetics of evolution of the more stable phases at 913 K, where Al and TiC do not coexist in thermodynamic equilibrium, were investigated in the present work. Preliminary results of this investigation were reported previously.[17] Substantial increases in Young's modulus and strength properties from the solid state reactions were observed, but there was a decrease in ductility. A component made by forming highly ductile XD Al/TiC composite may be heat-treated to give much higher stiffness, hardness, and strength. This may be a route to developing a useful high modulus aluminum alloy based composite.

II. MATERIAL

The composites for this investigation prepared by the ingot metallurgy XD process were obtained from Martin Marietta Laboratories and had 15 vol.% TiC dispersions with 0.7 ± 0.3 μm or 4.0 ± 2.0 μm particle size. Both composites were prepared by the two step XD exothermic dispersion process.[18] First, TiC was precipitated *in situ* in molten aluminum to form a "master alloy" with a high volume fraction of TiC. Then, the XD master alloy was diluted with 99.99% pure aluminum and cast into a 75 mm diameter mold. The ingots were extruded at 648 K with a 27:1 extrusion ratio to 12.5 mm diameter. The composite with 0.7 μm particle size also had 0.5 vol.% Al_3Ti particles which formed from excess titanium by a peritectic reaction.

III. EXPERIMENTAL

The as-received samples containing 0.7 μm TiC particles were held at 913 K for 24 to 496 h in a flowing argon environment. The 4.0 μm particle size composite was heat-treated for 168 to 336 h. The temperature chosen for heat treatment is 0.97 T_m and solid state diffusion rates are expected to be rapid. The as-extruded

and heat-treated samples were studied using a scanning electron microscope with energy dispersive x-ray analysis (EDAX), an x-ray diffractometer with a Cu K_α target tube, and a Hitachi H-700H transmission electron microscope (TEM) at an operating voltage of 200 kV. The specimens for TEM were prepared by mechanical polishing to a thickness of 10 μm, followed by argon ion thinning using a liquid nitrogen cooled stage.

The microhardness values at room temperature were measured using a Vicker's diamond indenter at loads of 500 g and 1 kg. High temperature hardness measurements were performed using a Vicker's diamond indenter in an argon environment at temperatures in the range of 0.5 to 0.8 T_m of Al. Young's moduli were determined dynamically by measuring the longitudinal vibration resonant frequency of a composite oscillator consisting of a quartz crystal to which a matched sample was cemented. Knowing the resonant frequency of the quartz crystal (75 kHz), the resonant frequency of the sample, f, was determined and the modulus, E, calculated by the well-known equation,[19] $E = 4l^2\rho f^2/n^2$, where l is the length of the sample, n is an integer (1 for the first harmonic, the present case), and ρ is the density.

Both as-received (extruded at 648 K) and 24 h 913 K heat-treated samples were cold rolled to a reduction of 75% and examined to determine the behavior of the interface during deformation.

Room and high temperature (536 and 698 K) tension tests were conducted on selected samples of the 0.7 μm TiC particle size composite. Prior to tensile testing, the as-extruded samples were annealed at 623 K for half an hour to relax any residual stresses due to extrusion and thermal expansion mismatch (about 4 : 1) between Al and TiC and produce a lower energy dislocation structure. The strain rate was 10^{-3} per second. The high temperature tension tests at 698 K were carried out in vacuum (10^{-4} Torr).

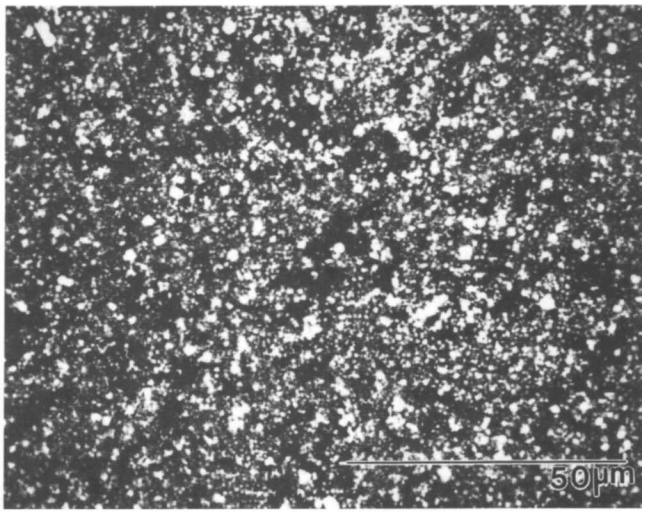

(a)

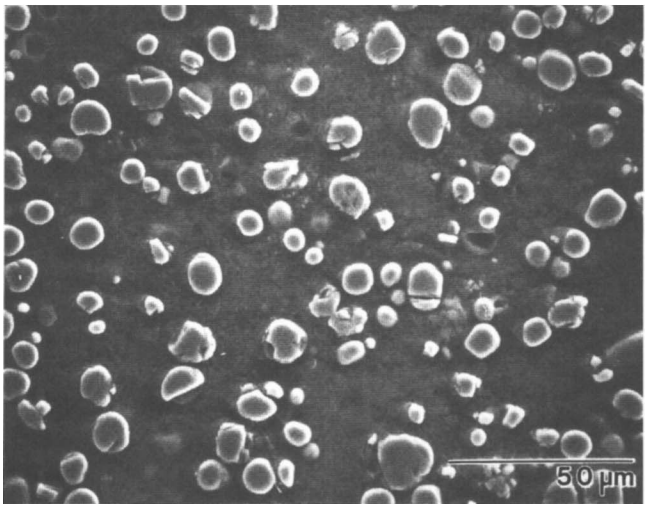

(b)

FIG. 1. SEM micrograph of Al/TiC composite in as-extruded form with (a) 0.7 μm particle size and (b) 4.0 μm particle size.

IV. RESULTS AND DISCUSSION

The changes observed in microstructure and the mechanical properties are discussed in the following and correlated with the available thermodynamic data.

A. SEM microstructural examination

Figures 1(a) and 1(b) show SEM micrographs of as-extruded Al/TiC composite with the different particle sizes. The interface is atomically abrupt after XD processing and extrusion, as clearly shown in the atomic resolution TEM image of the interface in Fig. 2.[16] The sample with 0.7 μm particle size underwent a large change in the microstructure with increase in heat-treatment time at 913 K, as shown in Figs. 3(a) and 3(b). Emergence of large particles with high aspect ratios is seen and the volume fraction of the dispersed phases increases with time of heat treatment. Changes were also observed in the 4.0 μm particle size composite, but they are mostly restricted to the interface. This is shown in Fig. 4, which is a micrograph of a sample heat-treated for 264 h. The composition of the reaction product labeled "X" determined from EDAX analysis is Al_3Ti. The reaction is limited to the interfacial region because the diffusion distances are longer and the bigger TiC particles have less surface-to-volume ratio. Figure 5 shows an SEM backscattered image of a 0.7 μm particle size sample after 336 h at 913 K. The light shaded particles in Fig. 5 again are Al_3Ti according to EDAX analysis. The dark shaded particles marked D in Figs. 4 and 5 are likely Al_4C_3 since they have an average atomic number lower than that of Al, the matrix phase.

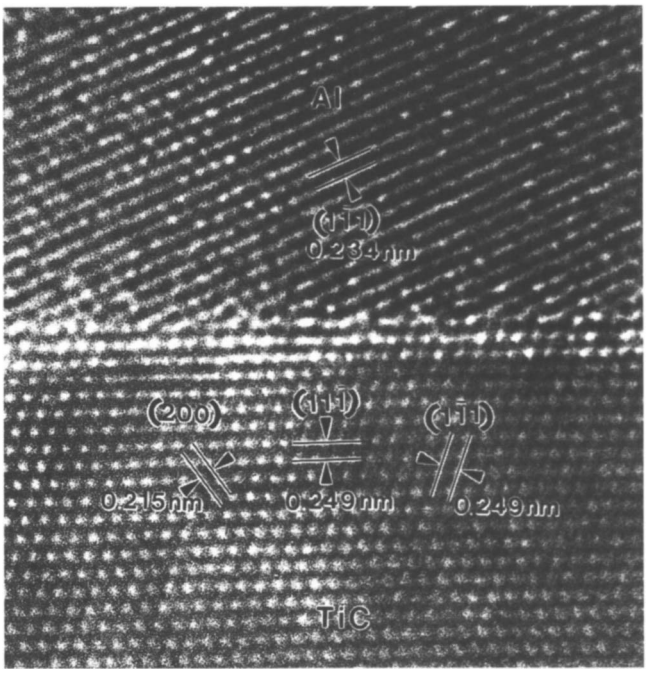

FIG. 2. HRTEM image of an Al/TiC interface in the as-extruded 0.7 μm particle size composite showing that it is abrupt on an atomic size scale.

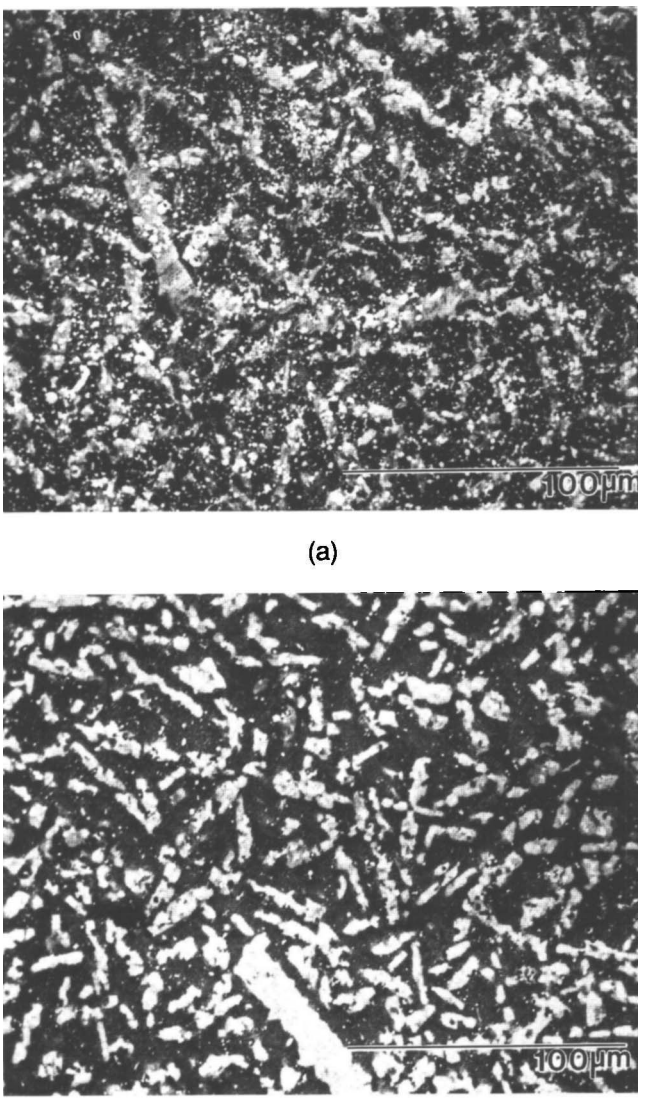

FIG. 3. SEM micrographs of the composite with 0.7 μm particle size heat-treated at 913 K: (a) 96 h and (b) 336 h.

B. TEM analysis

Figures 6–9 show TEM micrographs of the different phases resulting from thermal treatment; Al_3Ti and Al_4C_3 are the major product dispersed phases observed. Figure 6(a) shows a bright-field micrograph of an Al_3Ti particle formed by heat treatment for 24 h at 913 K. The particle was positively identified by electron diffraction. Dislocations evident in the figure are commonly seen in the Al_3Ti particles. Further heat treatment (96 h) increases the average particle aspect ratio. An example is shown in the dark-field TEM micrograph, Fig. 6(b). Most Al_3Ti particles have TiC particles embedded inside them.

A particle of Al_4C_3 is shown in Fig. 7(a). The (006), (012), and (018) spots of Al_4C_3 are identified in the electron diffraction pattern Fig. 7(b). EELS analysis also identified this and similar particles as Al_4C_3. Most of the Al_4C_3 particles have high aspect ratios. Two other phases, TiAl and Ti_2AlC, were also identified by electron diffraction after thermal treatment at 913 K in the 0.7 μm TiC/Al composite. Figure 8 shows a dark-field micrograph of a TiAl particle in a sample heat-treated for 336 h. The TiAl particles are irregular-shaped with an aspect ratio of about 3 and are several microns in length. Many TiC particles contain faults such as in the particle shown. The TiAl phase appears to have formed on TiC particles. Dislocations can also be seen. Figure 9 shows a dark-field micrograph of a Ti_2AlC particle in a sample also heat-treated for 336 h. The Ti_2AlC particles are also faulted and are hexagonal in cross section, with a large aspect ratio. Again the Ti_2AlC is usually associated with TiC.

C. X-ray diffraction analysis

X-ray diffraction results for the heat-treated 0.7 μm particle size Al/TiC composite are shown in Fig. 10. An angular range of 30°–50° is shown as this contained the maximum intensity peaks for all the phases present. In the as-extruded only Al and TiC peaks are shown. On 915 K exposure, the intensities of the Al peaks decrease, while diffraction peaks of Al_3Ti, Al_4C_3, and Ti_2AlC show up. Overlapping of major peaks of Al, TiAl, Al_3Ti, and Ti_2AlC makes interpretation of peak

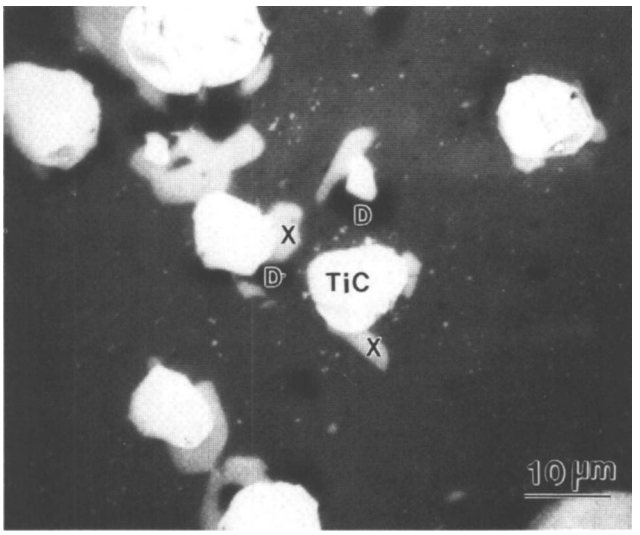

FIG. 4. Backscattered SEM image of composite with 4.0 μm particle size after heat-treating for 264 h. EDAX spectrum from spots "X" showed that the lighter reaction product is Al_3Ti. The region darker than matrix is labeled "D" and is believed to be Al_4C_3.

heights difficult. Surprisingly, the intensity of the Al_4C_3 peaks is low.

The position of the TiC peaks changes with heat treatment toward smaller *d* spacings, suggesting that TiC loses carbon. This is illustrated in Fig. 11 where a high index (422) TiC peak is shown that is not affected by any other neighboring peak. After 168 h at 913 K, peak broadening is observed. For longer periods of heat treatment, besides decrease in integrated intensity and broadening, shifts in TiC peak positions toward larger Bragg angle can be seen. The changes in intensity,

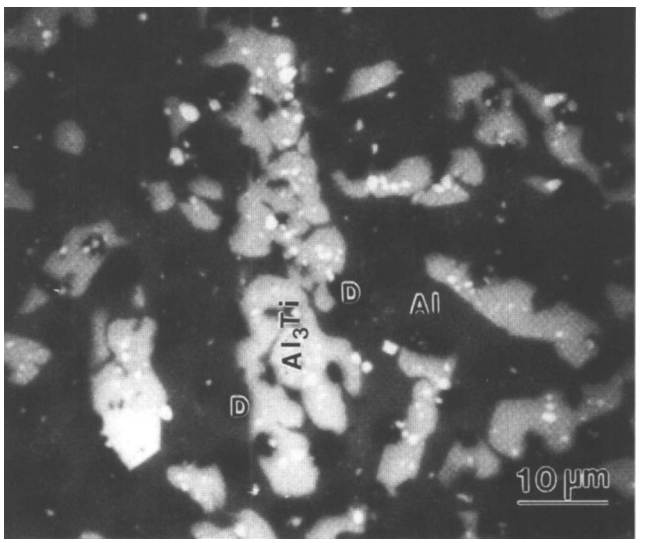

FIG. 5. Backscattered SEM image of composite with 0.7 μm particle size after heat-treating for 336 h. The light elongated particle marked according to the EDAX spectrum is Al_3Ti. The darker regions labeled "D" are believed to be Al_4C_3.

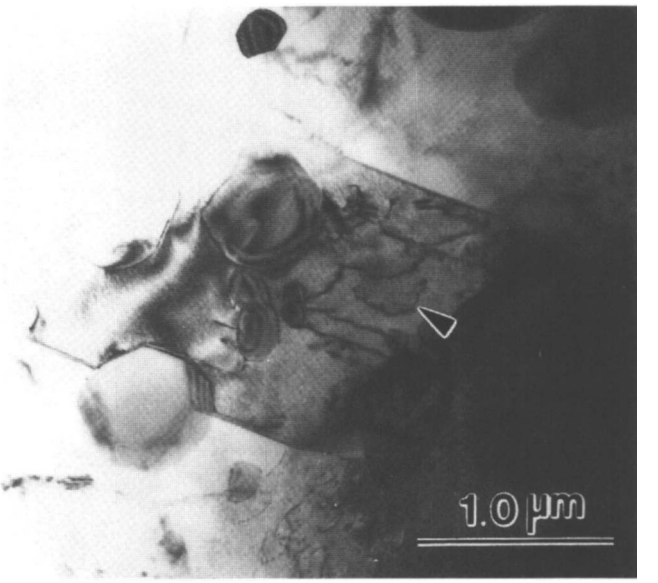

(a)

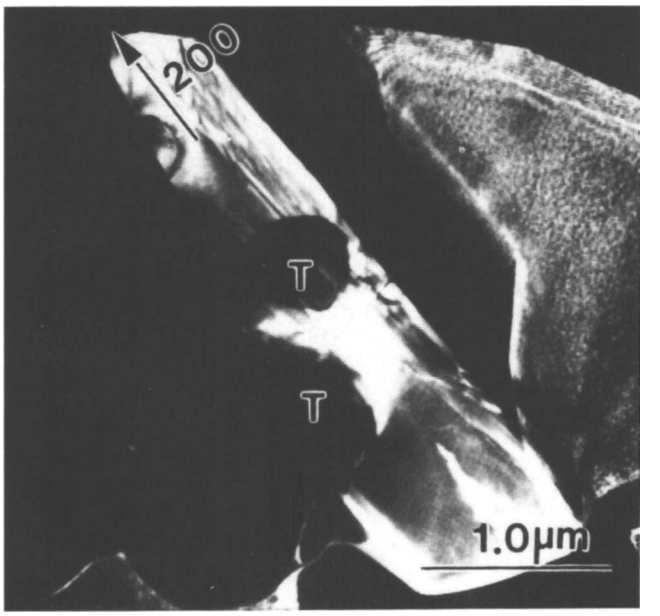

(b)

FIG. 6. Al_3Ti particles identified by electron diffraction pattern: (a) bright-field TEM micrograph from sample heat-treated at 913 K for 24 h showing dislocations (arrowed) and (b) TEM micrograph showing a particle with a high aspect ratio in a sample heat-treated for 96 h. Unreacted TiC particles are marked by "T".

peak shape, and position are also observed in other TiC peaks. This indicates that the lattice parameter changes with time at 913 K, as previously seen by Konitzer and Loretto[20] at a higher temperature. TiC can exist in the same crystal structure with atomic percentage of carbon varying between 33% and 48%.[21] TiC evidently becomes substoichiometric leading to a decrease in lattice parameter.

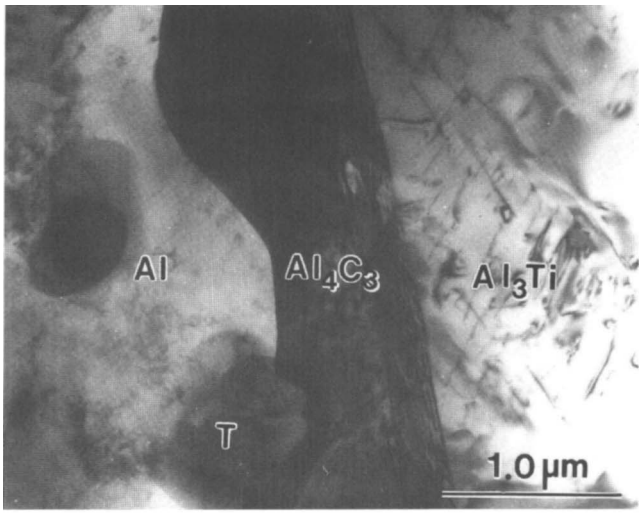

(a)

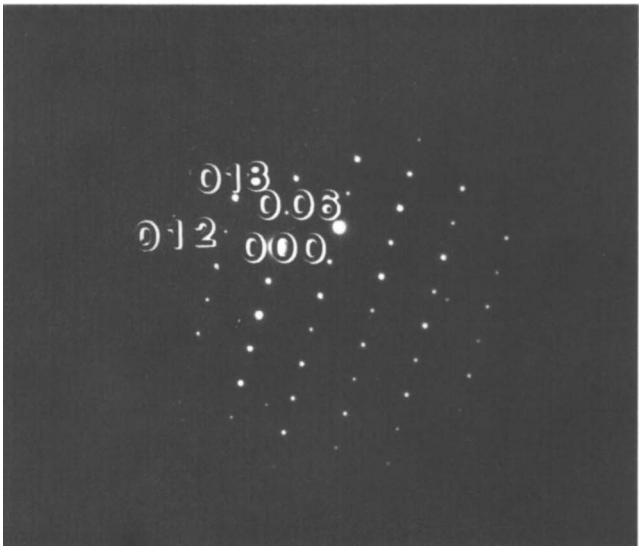

(b)

FIG. 7. Al_4C_3 particle: (b) electron diffraction pattern and (a) bright-field TEM micrograph. Sample heat-treated at 913 K for 24 h. Unreacted TiC particles are marked by "T".

Figure 12 shows the x-ray diffraction patterns of the 4.0 μm particle size composite heat-treated for 264 h at 913 K; Al_3Ti and Al_4C_3 peaks can be seen. None was seen before heat treatment. The Al_3Ti and Al_4C_3 peak heights are small compared to Al and TiC even for long heat treatment, correlating the slower reaction for bigger particles.

D. Thermodynamic analysis

Figure 13 shows free energy versus temperature curves for reactions[22]:

$$3TiC + 13Al(1/s) = Al_4C_3 + 3Al_3Ti \quad (1)$$

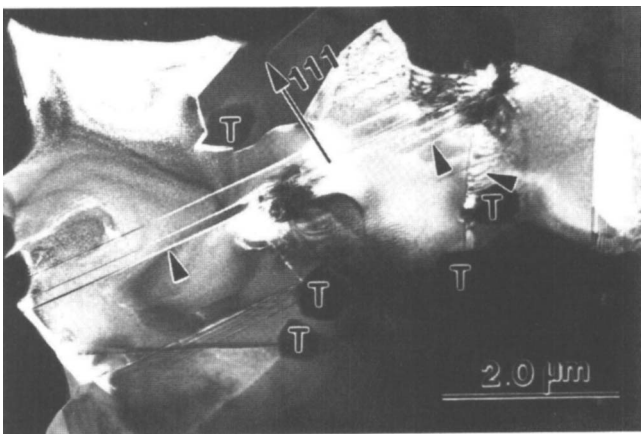

FIG. 8. Dark-field TEM micrograph of a TiAl particle from a sample heat-treated for 336 h at 913 K. Stacking faults and dislocations are seen. Unreacted TiC particles are marked by "T".

$$3TiC + 7Al(1/s) = Al_4C_3 + 3TiAl \quad (2)$$

$$3TiC + 4Al(1/s) = Al_4C_3 + 3Ti \quad (3)$$

Reaction (1) proceeds to the right only below 1025 K, above which the free energy change for the reaction is positive. The presence of Al_3Ti and Al_4C_3 after heat-treating at 913 K is expected. Reactions (2) and (3) have positive free energy changes at all temperatures. Reaction (1) has been discussed previously by Yokokawa *et al.*[8] and Satyaprasad *et al.*[11]

The evolution of the microstructure can be discussed further using the ternary Al–Ti–C phase diagram in Fig. 14 drawn for 913 K from the binary phase diagrams

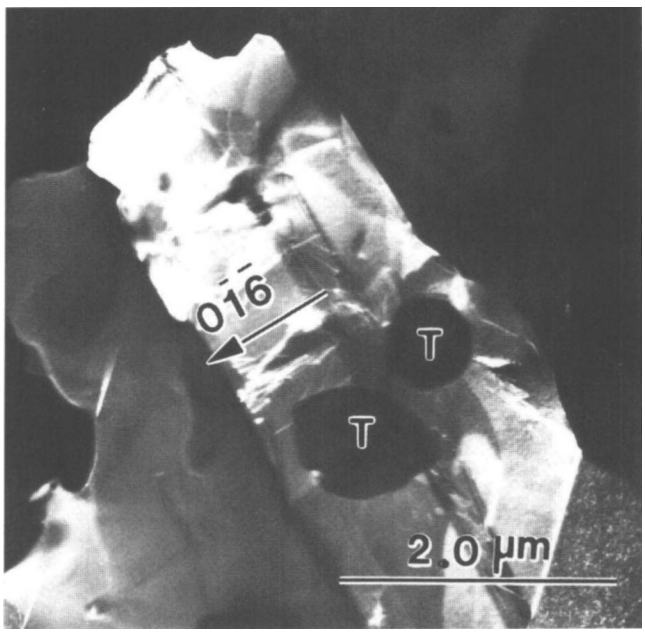

FIG. 9. Dark-field TEM micrograph of a Ti_2AlC particle from a sample heat-treated for 336 h at 913 K. TiC particles are marked by "T".

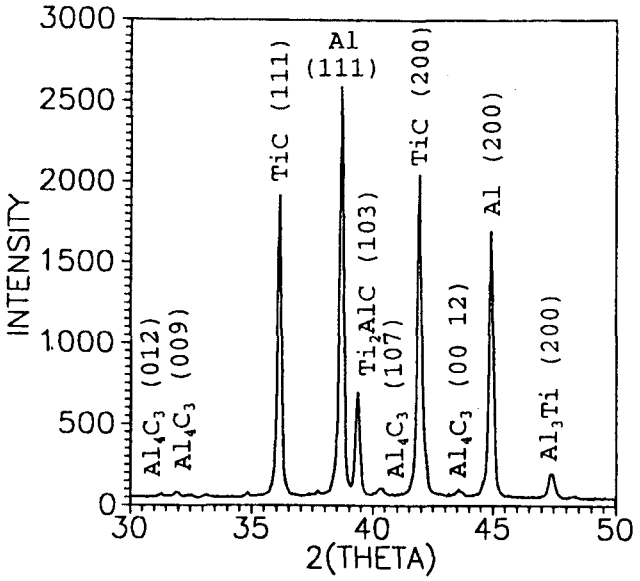

FIG. 10. X-ray diffraction patterns in the range of 30°–50° for samples with 0.7 μm particle size composites heat-treated at 913 K for 24 h.

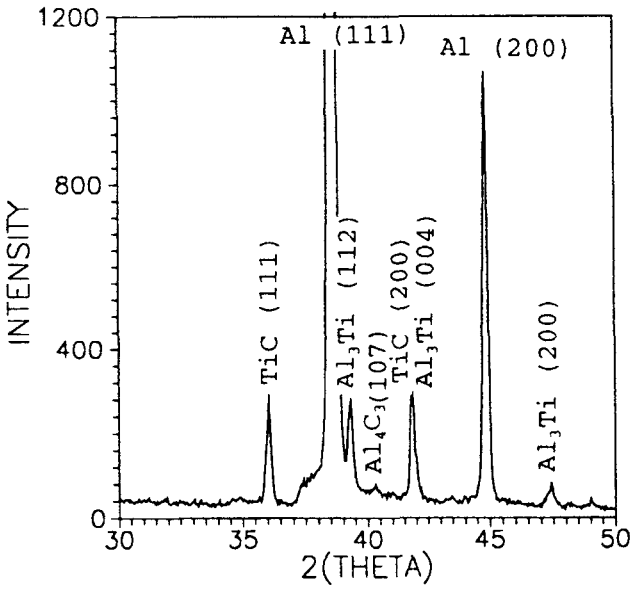

FIG. 12. X-ray diffraction pattern in the range 30°–50° for samples with 4.0 μm particle size composites heat-treated at 913 K for 264 h.

of the Al–C, Ti–C, and Al–Ti systems[23] and the ternary phase diagram[17,18] at 1023 K which is just above T_m of Al. The ternary compounds H (Ti_2AlC) and P (Ti_3AlC) were assumed not to change on cooling to 913 K. Tie-lines between coexisting phases have been drawn using information from Fig. 13. TiAl and Al_4C_3 are not joined, as Eq. (2) shows that they react to form Al and TiC at 913 K. Also, the chemical reaction

$$13TiAl + 2Al_4C_3 = 6TiC + Al_3Ti \qquad (4)$$

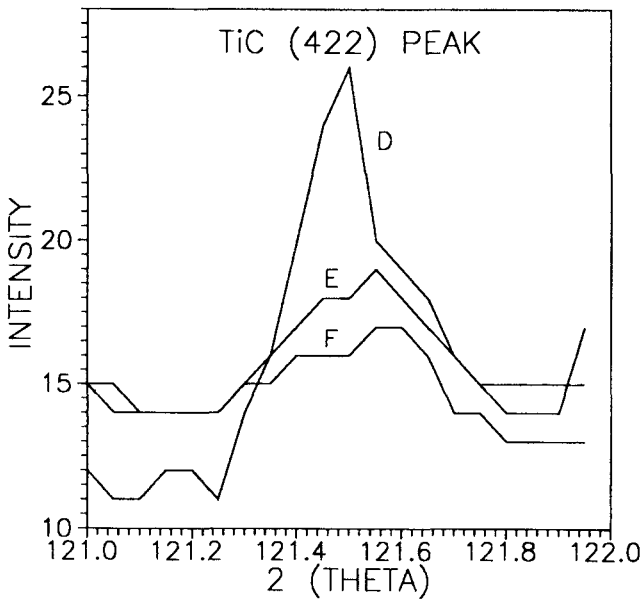

FIG. 11. X-ray diffraction pattern showing (422) TiC peak position and shape changes with time of heat treatment at 913 K showing peaks for (D) 168 h, (E) 328 h, and (F) 496 h heat treatment.

has a negative free energy change up to temperatures higher than 5000 K,[5,17] predicting that TiC and Al_3Ti coexist. Similarly, Ti_3Al and Al_4C_3 are not joined. The present calculations agree well with the corrected partial phase diagram of Norman *et al.*[5] and the predictions from the three-dimensional chemical potential diagrams of Al–Ti–C system drawn by Yokokawa *et al.*[8] for 973 K.

The composition in the present case lies in triangle I in Fig. 14, where Al, Al_3Ti, and Al_4C_3 are the stable phases. The formation of TiAl is puzzling. Because of inhomogeneities, there may be local regions where the

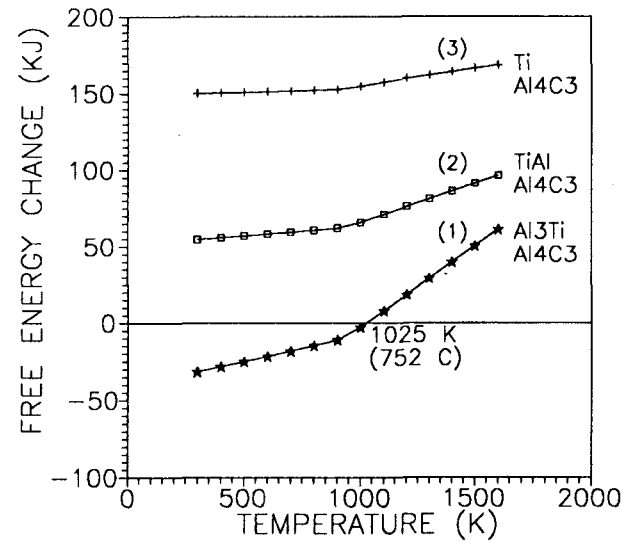

FIG. 13. Free energy versus temperature plots for reactions (1)–(3).

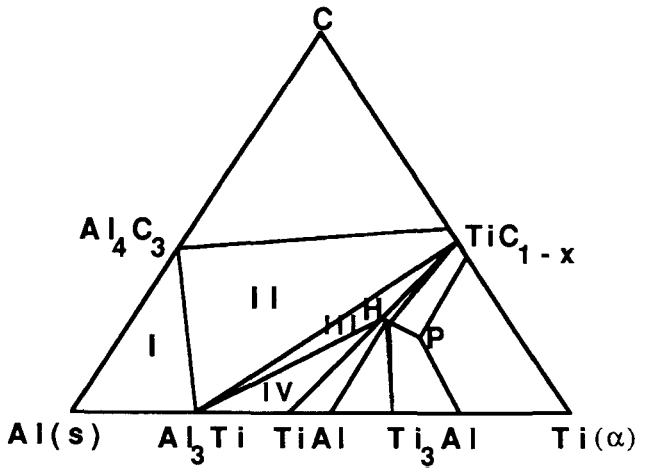

FIG. 14. Isothermal ternary Al–Ti–C phase diagram at 913 K.

compositions lie in triangles II, III, or IV giving rise to TiAl and Ti_2AlC.

E. Mechanical property changes

1. Microhardness

The room temperature microhardness values of the Al/TiC composite for both particle sizes are plotted against time at 913 K in Fig. 15. The hardness of the 0.7 μm composite increases monotonically and after 496 h is more than 4 times the hardness of the as-extruded composite. Similar but much smaller increases are also observed in the 4.0 μm particle size composite. The hardness increases are due to the increase in volume fraction of intermetallics from the chemical reaction between Al and TiC. Both composites were also heat-treated at 773 K for the same amounts of time and, as shown in Fig. 15, no change in room temperature hardness was observed. The microstructure did not show any observable change at this temperature because the kinetic barriers are evidently too high at this temperature, even though 773 K is 0.83 T_m of Al.

High temperature hardness values are plotted in Figs. 16(a) and 16(b) for the 0.7 μm Al/TiC composite. The 913 K heat-treated samples again proved to be much stronger compared to the as-received composite at all temperatures up to 723 K (0.8 T_m). The hardness at all temperatures increased with aging time. The high volume fraction of hard intermetallic particles in the microstructure after aging raises the hardness at high temperatures as well as at room temperature. Interest-

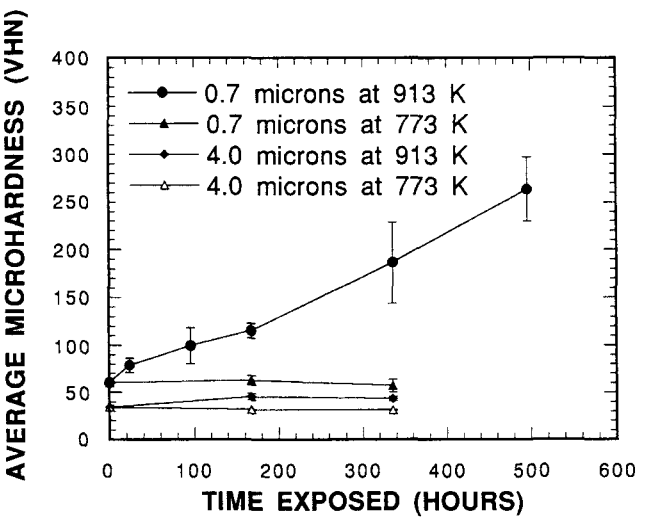

FIG. 15. Plot of room temperature hardness of composites with 0.7 and 4.0 μm particle sizes for heat treatment at 913 and 773 K for different periods of time.

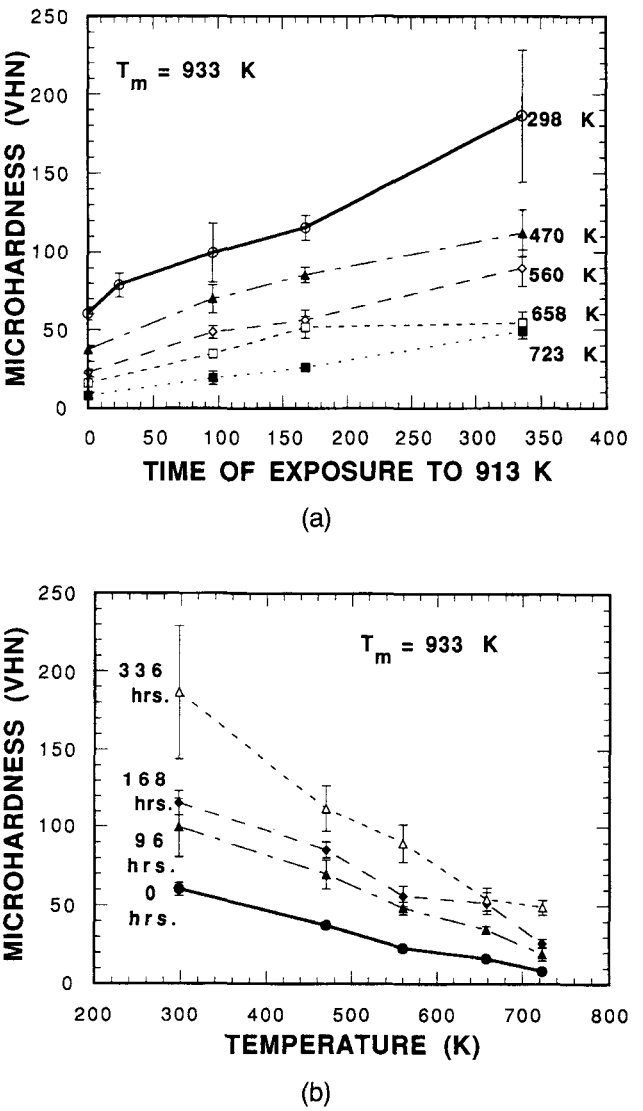

FIG. 16. High temperature hardness behavior of Al/TiC composite containing 0.7 μm particles: (a) dependence of microhardness at various temperatures on the time of heat treatment at 913 K; (b) temperature dependence of microhardness, samples held at 913 K for various lengths of time.

ingly, the hardness after 336 h of aging at 913 K is almost the same at 658 K as that at 723 K.

2. Young's modulus

Young's moduli for the composites with both particle sizes are plotted against time at 913 K in Fig. 17. The modulus increases for both particle sizes, but the change is far more significant for the smaller particle size. After 336 h at 913 K, a modulus increase of about 50% to 142 GPa is observed for the 0.7 μm TiC composite. This is a significant increase which should be of technological interest.

3. Tension tests

The room temperature engineering stress-strain curves for the 0.7 μm particle size composite heat-treated 0 h (as-extruded and stress relieved), 24, 48, and 96 h at 913 K are shown in Fig. 18. Figure 19 shows the yield and ultimate tensile strength and elongation versus time at 913 K. The yield and ultimate tensile strengths increase and the ductility decreases with increasing heat-treatment time. The effect of heat treatment on the strength is much smaller after the first 24 h.

Tension tests were also done on the 0.7 μm particle size composite at 536 and 698 K (Tables I and II). The strength of the as-received (extruded and stress-relieved) Al/TiC falls considerably on heating. The strength of the heat-treated samples falls less. The UTS of the latter is more than twice that of the former at 536 K as well as at 698 K. The ductilities as measured by percentage elongation are significantly larger at 698 K compared with those at room temperature or 536 K, but there is a substantial drop in strength.

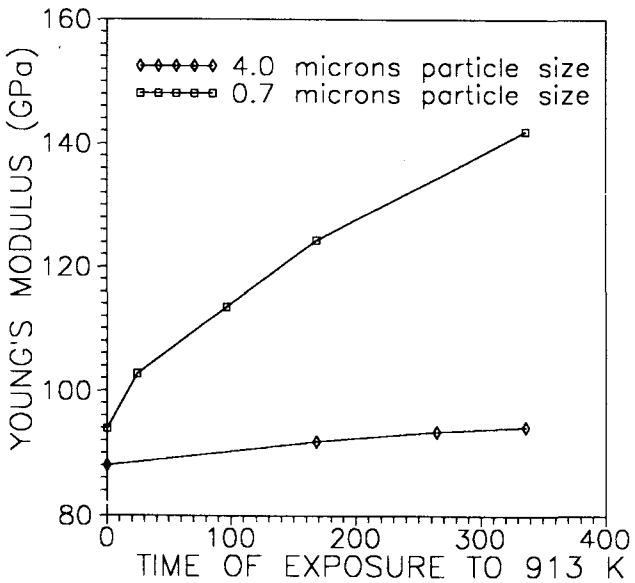

FIG. 17. Young's modulus versus time of heat treatment at 913 K for composites with 0.7 and 4.0 μm particle sizes.

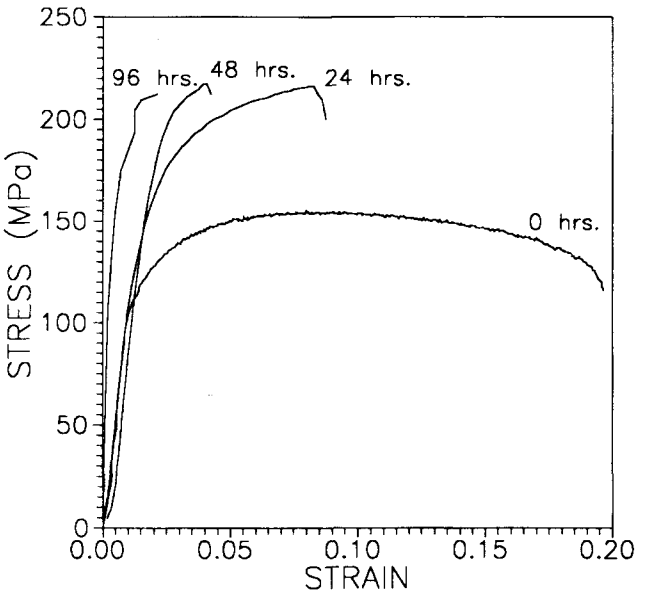

FIG. 18. Room temperature engineering stress-strain curves for 0.7 μm particle size composite for periods of heat treatment up to 96 h. The decrease in elongation to failure can be clearly seen.

4. Comparison of fracture mechanisms

Samples of the as-extruded and 24 h heat-treated Al–0.7 μm TiC composite were cold rolled and examined in the TEM. In the case of as-extruded composite, the Al–TiC interfaces were essentially without any cracks even after 75% reduction in thickness without intermittent annealing, as shown in Fig. 20(a). The sharp clean interface present in the as-received composite has good ductile bonding. The deformation mechanism near the interface is by local lattice rotation.[24] A cell structure is formed by recovery in the Al matrix during deformation. Small voids are seen only in regions where TiC particles are clustered. On heat-treating 24 h

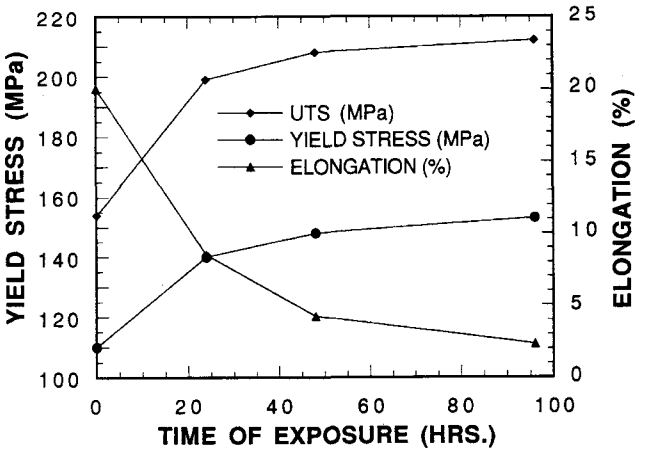

FIG. 19. Variation of room temperature strength (yield and ultimate tensile strength) and elongation to failure with time of heat treatment at 913 K, respectively.

TABLE I. Tension test data of Al/15 vol. % TiC composite (0.7 μm initial particle size) at 536 K (0.58 T_m).

Specimen type	Y.S. (MPa)	UTS (MPa)	Elong. (%)
As-extruded and annealed	78.0	83.3	35.0
Heat-treated for 96 h	150.0	180.8	4.0
Heat-treated for 336 h	191.0	193.5	1.0

at 913 K, most interfaces containing reaction products appeared cracked after cold rolling to 75% reduction. This can be seen in Fig. 21. Fracture surfaces of 0.7 μm composite specimens without any heat treatment and after heat treatment at 913 K tested at room temperature were examined. More particles were seen in the dimples on the fracture surface of the heat-treated composite, showing evidence of more debonding. Fracture surfaces after testing at 698 K show an increase in dimple size correlating with increase in elongation.

The Al_3Ti particles in the just heat-treated microstructure show dislocation structures, as shown in Fig. 6(c). These dislocations become mobile on heating leading to improved deformability in Al_3Ti at elevated temperatures but lower strength.

F. Suggested practical use

The Al/TiC composite is very ductile and can be mechanically formed by hot working or cold working to the desired shape and then heat-treated to substantially increase modulus but with decrease in ductility. For the present study of the TiC–Al interface reaction, unalloyed Al was chosen for the matrix to avoid complications. Any technological development of this concept would use an alloy matrix to increase the yield and tensile strengths. A study conducted by Jangg *et al.*[25] on Al/Al_4C_3 composite has shown little difference with corrosion properties of unreinforced Al. Hence, Al_4C_3 formation may not create a corrosion problem.

V. FINAL DISCUSSION AND CONCLUSIONS

(1) Even though Al and TiC co-exist in equilibrium at high temperatures, this changes on cooling so that thermal exposure of the Al/TiC composite at 913 K leads to the chemical reaction $13Al + 3TiC = 3Al_3Ti + Al_4C_3$. Thermodynamic considerations show that the reaction has a negative free energy change at temperatures below 1025 K. Equilibrium ternary Al–Ti–C phase diagrams drawn for 913 K in this work and for 1023 K,[17] respectively, show coexistence of Al, Al_3Ti, and Al_4C_3 for the present composition.

(2) The phases TiAl and Ti_2AlC also appeared in certain areas in the sample with 0.7 μm particle size. This was determined by TEM and x-ray diffraction. Their appearance can be due to localized compositional variations caused by uneven distribution of TiC.

(3) It is safe to process (anneal or hot work) Al–TiC composites in the solid state at 773 K or somewhat higher where the reaction kinetics are very slow.

TABLE II. Tension test data at 698 K (0.75 T_m).

Specimen type	Y.S. (MPa)	(MPa)	Elong. (%)
As-extruded and annealed	21.0	32.1	56.0
Heat-treated for 96 h	31.0	75.0	10.0

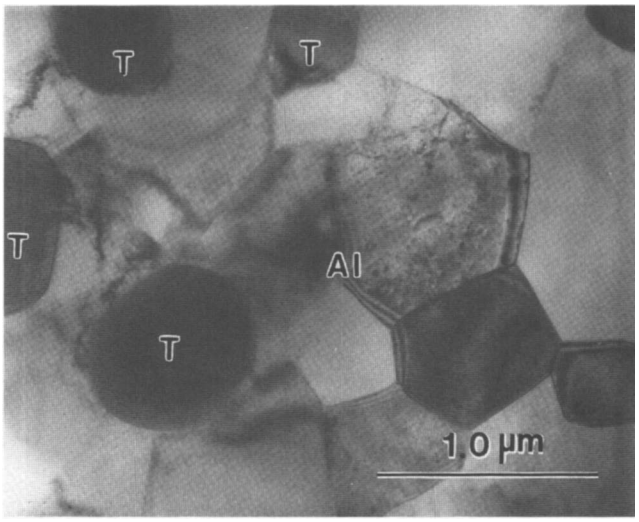

FIG. 20. TEM micrograph showing interfaces in as-received 0.7 μm particle size Al/TiC composite after cold rolling. The particle-matrix interfaces are without cracks. A cell structure develops in the matrix during deformation.

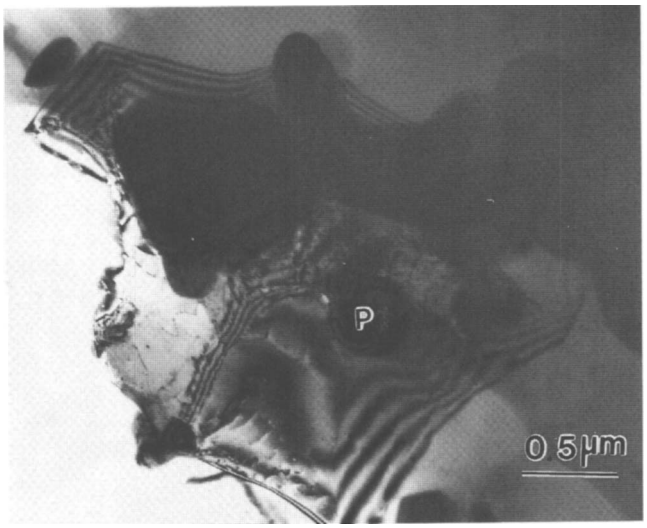

FIG. 21. TEM micrograph showing a representative region of an interface between TiC (marked "T") and reaction products cracked during rolling in a sample heat-treated for 24 h at 913 K. Cracks are normally sharp.

(4) Microstructural changes obtained by heat treatment at 913 K for the submicron particle size composite have resulted in a substantial increase in stiffness.

(5) The XD Al/TiC composite is very ductile in the as-extruded condition and can be cold or hot worked into useful components and then heat-treated appropriately to improve stiffness.

ACKNOWLEDGMENTS

This research was supported by the Air Force Office of Scientific Research, Grant No. AFOSR-89-0043, under the direction of Dr. Alan Rosenstein. The authors wish to acknowledge R. M. Aikin, Jr. of Martin Marietta Laboratory, Baltimore, Maryland for the XD Al/TiC composites and useful discussions. Thanks are also due to Professor K. T. Faber for permission to use the high temperature hardness tester. Use was made of the central facilities supported by the MRL program of NSF, Grant No. NSF DMR-8821571. The authors are also grateful to Mr. M. Seniw of Northwestern University Mechanical Testing Facility and Dr. W. A. Chiou of the TEM facility for extending their helping hands whenever needed.

REFERENCES

1. K. K. Chawla, *Composite Materials Science and Engineering* (MRE Series, Springer-Verlag, Berlin, 1987), p. 102.
2. C. G. Rhodes and R. A. Spurling, in *Developments in Ceramic and Metal-Matrix Composites*, edited by K. Upadhya (TMS, Warrendale, PA, 1992), p. 99.
3. R. B. Clough, F. S. Biancaniello, H. N. G. Wadley, and U. R. Kattner, Metall. Trans. **21A**, 2747 (1990).
4. J. C. Schuster, H. Nowotny, and C. Vaccaro, J. Solid State Chem. **32**, 213 (1980).
5. J. H. Norman, G. H. Reynolds, and L. Brewer, in *Intermetallic Matrix Composites*, edited by D. L. Anton, P. L. Martin, D. B. Miracle, and R. McMeeking (Mater. Res. Soc. Symp. Proc. **194**, Pittsburgh, PA, 1990), p. 369.
6. M. E. Fine and J. G. Conley, Metall. Trans. **21A**, 2609 (1990).
7. R. A. Rapp and X. Zheng, Metall. Trans. **22A**, 3071 (1991).
8. H. Yokokawa, N. Sakai, T. Kawada, and M. Dokiya, Metall. Trans. **22A**, 3075 (1991).
9. A. Banerji and W. Reif, Metall. Trans. **17A**, 2127 (1986).
10. A. Jafors, H. Fredriksson, and L. Froyen, Mater. Sci. Eng. **A135**, 119 (1991).
11. K. Satyaprasad, Y. R. Mahajan, and V. V. Bhanuprasad, Scripta Metall. **26**, 711 (1992).
12. D. Lewis III, in *Metal Matrix Composites: Processing and Interfaces*, edited by R. K. Everett and R. J. Arsenault (Academic Press, San Diego, CA, 1991), p. 141.
13. P. Sahoo and M. J. Koczak, Mater. Sci. Eng. **A144**, 37 (1991).
14. M. K. Premkumar and M. G. Chu, in *Development of Ceramic and Metal-Matrix Composites*, edited by K. Upadhya (TMS, Warrendale, PA, 1992), p. 323.
15. A. R. C. Westwood, Metall. Trans. **19A**, 749 (1988).
16. R. Mitra, W. A. Chiou, J. R. Weertman, M. E. Fine, and R. M. Aikin, Jr., Scripta Metall. **25**, 2689 (1991).
17. R. Mitra, J. R. Weertman, M. E. Fine, and R. M. Aikin, Jr., in *Development of Ceramic and Metal Matrix Composites*, edited by K. Upadhya (TMS, Warrendale, PA, 1992), p. 125.
18. R. M. Aikin, Jr., Martin Marietta Laboratory, private communication.
19. M. E. Fine, in *Symposium on Determination of Elastic Constants* (Am. Soc. Test. Mater., Philadelphia, PA, 1952), ASTM STP **129**, 1.
20. D. G. Konitzer and M. H. Loretto, Acta Metall. **37**, 397 (1989).
21. H. Goretzki, Phys. Status Solidi **20**, K141 (1967).
22. I. Barin, *Thermochemical Data of Pure Substances* (VCH Publishers, Weinheim, Germany, 1989), pp. 17, 26, 71, 72, 1520, 1528.
23. P. R. Sherry and M. H. Bankard, in *ASM Metals Handbook–Metallography, Structures and Phase Diagrams*, edited by T. Lyman (Metals Park, OH, 1973), Vol. 8, p. 120.
24. F. J. Humphreys, in *Dislocations and Properties of Real Materials* (The Institute of Metals, London, 1985), p. 175.
25. G. Jangg, F. Kutner, and G. Korb, Powder Metall. Inter. **9**, 24 (1977).